Long-lived particle searches with the ILD experiment

Daniel Jeans[2], *Jan Franciszek* Klamka[1,*], and *Aleksander Filip* Żarnecki[1]

[1]Faculty of Physics, University of Warsaw, Pasteura 5, 02-093 Warsaw, Poland
[2]KEK, 1-1 Oho Tsukuba, Ibaraki 305-0801, Japan

Abstract. Future e^+e^- colliders provide a unique opportunity for long-lived particle (LLP) searches. This study focusses on LLP searches using the International Large Detector (ILD), a detector concept for a future Higgs factory. The signature considered is a displaced vertex inside the ILD's Time Projection Chamber. We study challenging scenarios involving small mass splittings between heavy LLP and dark matter, resulting in soft displaced tracks. As an opposite case, we explore light pseudoscalar LLPs decaying to boosted, nearly collinear tracks. Backgrounds from beam-induced processes and physical events are considered. Various tracking system designs and their impact on LLP reconstruction are discussed. Assuming a single displaced vertex signature, model-independent limits on signal production cross section are presented for a range of LLP lifetimes, masses, and mass splittings. The limits can be used for constraining specific models, with more complex displaced vertex signatures.

1 Introduction

Despite the remarkable success of the Standard Model (SM) of particle physics, many phenomena, such as the existence of dark matter, baryon asymmetry, or the origin of neutrino masses, remain unexplained by the theory. However, no direct observation of any physics Beyond the Standard Model (BSM) has been made so far, regardless of numerous searches at the Large Hadron Collider (LHC) or other experiments.

An interesting concept that could explain why the new physics evades detection is a potential existence of BSM long-lived particles (LLPs). Such states, just like many particles in the SM, could travel macroscopic distances before decaying, making it very challenging to observe them. This idea gained a lot of interest in the last years, as the LLPs can naturally appear in many BSM models and be characterised by a range of very distinct signatures [1]. Experiments at the LHC performed a large number of searches for LLPs using many new interesting techniques and signatures. However, the main mechanisms responsible for an enhancement of particle lifetime include reduced couplings to the SM sector or small mass differences in a particle decay chain [2]. This, by definition, makes it very difficult to search for such states in the busy environment of a hadron collider.

According to the last 2020 Update of the European Strategy for Particle Physics, an e^+e^- Higgs factory is "the highest-priority next collider" [3]. Currently, there are several proposals for such a machine, and the most mature concept is The International Linear Collider

*e-mail: jan.klamka@fuw.edu.pl

(ILC) [4]. The triggerless operation and clean environment of a linear e^+e^- collider make it very promising in the context of searches for rare and exotic processes, such as LLP production. One of the experiments proposed for operation at a future Higgs factory is the International Large Detector (ILD) [5]. The ILD baseline design is optimized for event reconstruction with the particle-flow approach [6] based on highly granular calorimeters. The ILD tracking systems include a pixel vertex detector (VTX) and a silicon inner tracker (SIT), surrounded by a large time projection chamber (TPC). The TPC allows for almost continuous tracking, which is an excellent feature in the case of searches for delayed decays. For details about the ILD see Ref. [5] and references therein. This contribution is based on Ref. [7] and it presents prospects for detection of a neutral LLPs with the ILD, using ILC operating at $\sqrt{s} = 250\,\text{GeV}$ (ILC250) as a reference collider.

2 Analysis strategy and benchmark scenarios

The study is conducted from an experiment-oriented point of view. The aim was to test the ILD sensitivity to LLPs on the basis of its experimental features. Therefore, benchmark scenarios were not selected as preferred points in the parameter space of a particular BSM model. Instead, test scenarios involved challenging signatures that allow for testing capabilities and potential limitations of detectors and reconstruction techniques. As a signal of neutral LLP production, we consider a generic case of two tracks that form a displaced vertex; it is a conservative approach, as the so-called displaced jet signature (with more tracks in the final state) should be even more clean and easier to detect. No further assumptions are made about the final state, which allows one to keep the analysis model independent.

Two opposite classes of benchmarks are considered. The first one involves production of a heavy LLP, which leads to a signature of a very soft displaced track pair in the final state. Events for the analysis were generated in the framework of Inert Doublet Model [8], using pair-production of neutral heavy scalars, A and H, where the former is the LLP and the latter is stable (and escapes undetected). The LLP decay channel is $A \to Z^{(*)}H \to \mu\mu H$, with muons chosen to simplify the simulation process. The mass of LLP and the proper decay length were fixed to $m_A = 75\,\text{GeV}$ and $c\tau = 1\,\text{m}$, respectively. Four mass splitting values between A and H were considered: $m_A - m_H = 1, 2, 3, 5\,\text{GeV}$. The mass of A and the small mass splitting result in a very low transverse momentum of the final state.

The second class features exactly opposite case, i.e. production of a very light and highly boosted LLP, leading to a strong collimation of the final-state tracks. It was generated using the associated production of an axion-like particle [9], a pseudoscalar LLP, with a hard photon ($e^+e^- \to a\gamma$), again only with $a \to \mu\mu$ decays. Four masses of LLP were considered, $m_a = 0.3, 1, 3, 10\,\text{GeV}$, with the decay lengths $c\tau = 10 \cdot m_a\,\text{mm/GeV}$ to maintain large number of decays within the detector volume.

The analysis was based on a vertex-finding algorithm designed for the purpose of this study, which reconstructs the vertex in between the points of closest approach of track helices, if the distance between the points is smaller than 25 mm. The main assumption was to consider only the displaced vertex signature in the TPC, ignoring any other activity inside the detector. This allows one to perform the analysis as an "anomaly search" in a model-independent way, by looking for any excess in a number of vertices over the SM background. The study was carried out using full detector response simulation based on Geant4 [10], with iLCSoft v02-02-03 [11] used for reconstruction.

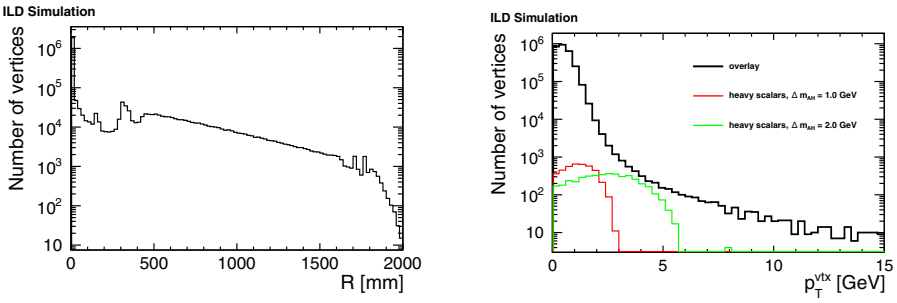

Figure 1: Left: Number of displaced vertices found in the overlay sample as a function of distance from the beam axis. Right: Total transverse momentum of tracks coming from a displaced vertex for the overlay (black) and scalar pair-production with $\Delta m_{AH} = 1$ GeV (red) and $\Delta m_{AH} = 2$ GeV (green). All histograms are normalized to the number of simulated events and correspond to no selection applied at all, just except for the required maximum distance between track helices.

3 Background reduction

Two types of background have been taken into account – soft, beam-induced (low-p_T) processes and hard (high-p_T) processes. At linear e^+e^- colliders, due to strong beam focusing, each bunch crossing (BX) is accompanied by $\gamma\gamma$ collisions, producing low-p_T hadrons and incoherent e^+e^- pairs. On average, 1.55 hadron photoproduction events and $O(10^5)$ incoherent pairs are expected at ILC250 per BX (where most of the latter are produced below the acceptance of the tracking system and only a small fraction might enter the tracker region). These so-called overlay events are typically analyzed in the context of hard processes (as they can occur in the detector simultaneously), but in some cases can constitute background on their own.

Figure 1 (left) presents a distribution of the vertices reconstructed by the algorithm in the overlay sample as a function of the distance from the beam axis. It shows there is a huge number of vertices, in particular close to the beam and to the inner wall of the TPC ($R \simeq 329$ mm), most of which are fake. In Fig. 1 the combined p_T^{vtx} of tracks forming a vertex in the overlay events is compared with the signal scenarios in the heavy scalar production case. Taking into account that $O(10^{11})$ BXs are expected per year at the ILC, this shows the beam-induced processes are a significant standalone background, if one wants to consider soft signals.

To reject fake vertices, a set of cuts was applied on the variables describing kinematic properties of tracks, such as their opening angle, number of hits, or a distance between the reconstructed displaced vertex and a first hit, relative to the track length. The main background sources that remain include long-lived neutral hadron decays (V^0 particles) and photon conversions, as well as secondary interactions of particles with the detector material. To suppress the V^0s, matching with a dedicated ILD software processor for V^0 identification is applied. However, due to a limited efficiency of the processor, further selection was needed. The invariant mass of a track pair system was calculated assuming that tracks are either both pions, one is a pion and the other is a proton, or both are electrons. Then, for the respective track mass hypotheses, vertices formed by tracks with an invariant mass corresponding to windows of ±50 MeV around K^0 and Λ^0 masses, and with a mass below 150 MeV (photon conversion) were rejected. Vertices created by interactions of charged particles with the detector are mitigated by restricting the search region to vertex radii in the 0.4-1.5 m range (i.e. inside the gas

Table 1: The vertex finding rates directly obtained for the high-p_T SM backgrounds inside the TPC region after different sets of cuts. Large statistical uncertainties for tight selection rates result from small number of MC events remaining after the selection.

background channel	qq	qqqq	$\gamma^{B/W}\gamma^{B/W}$
Finding rate (standard)	$(7.99 \pm 0.68) \cdot 10^{-4}$	$(1.486 \pm 0.094) \cdot 10^{-3}$	$(2.13 \pm 0.28) \cdot 10^{-5}$
Finding rate (tight)	$(2.30 \pm 1.15) \cdot 10^{-5}$	$(3.57 \pm 1.46) \cdot 10^{-5}$	$(1.06 \pm 0.61) \cdot 10^{-6}$

volume of the TPC) and by requirements related to impact parameter of tracks surrounding and forming the vertex.

Because it is not possible to generate event samples corresponding to the number of $O(10^{11})$ BXs expected in the real experiment, factorisation of the final selection was performed. Cuts were applied on variables that are not correlated, using event samples after the preliminary selection described above. Then, the total reduction factor can be obtained by multiplication of the individual cut efficiencies on two variables we used. The first was the total transverse momentum p_T^{vtx} of a pair of tracks, since the background is expected to occupy the region of very low p_T, as visible in Figure 1 (right). The second variable was a combination of a distance (in three dimensions) between track first hits in the TPC and a distance between centres of helix-circles (projections of track helices onto the XY plane) of the tracks. Cuts on these two variables, combined with the preliminary selection efficiency, give the total reduction factor of $1.26 \cdot 10^{-10}$.

The main background sources mentioned above happen predominantly inside the hadronic jets, therefore, in the case of hard processes we consider background channels with a hadron production: $q\bar{q}$, $q\bar{q}q\bar{q}$, $qq\ell\nu$, $qq\ell\ell$, $qq\nu\nu$, and a hard $\gamma\gamma$ scattering. As the vertex finding rates for these backgrounds were found to be dependent on the number of jets, rather than on the process itself, only the most significant channels ($q\bar{q}$, $q\bar{q}q\bar{q}$, and $\gamma\gamma$) were processed to directly obtain the reduction factors, in order to reduce the computational time. To further reduce background from coincidences of random tracks within high p_T hadronic jets, a separate cut on a distance between first hits of the tracks was applied in addition to the selection targeting beam-induced backgrounds described above. This whole set of cuts will be referred to as the *standard* selection.

To improve the background rejection and further reduce vertices from semileptonic K_L^0 decays and to photon conversions with poorly reconstructed, short tracks, we consider also a *tight* selection. In this case, the cuts on the invariant mass were enhanced, such that vertices with masses below 700 MeV are rejected for electron and pion track mass hypotheses. In addition, an isolation criterion was used, since most of the BSM scenarios predict the signal should be isolated, while vertices in the background samples are found mostly inside hadronic jets. The resulting vertex finding rates in the simulated background samples are summarized in Table 1, together with corresponding statistical uncertainties, for both standard and tight selection.

4 Results

Figure 2 presents the vertex finding efficiency after standard selection for two of the signal scenarios, heavy scalar pair-production with $\Delta m_{AH} = 2$ GeV (left) and for the light pseudoscalar production with $m_a = 1$ GeV (right). The efficiency is shown as a function of a true LLP decay vertex position inside the detector, where a reconstructed vertex was considered

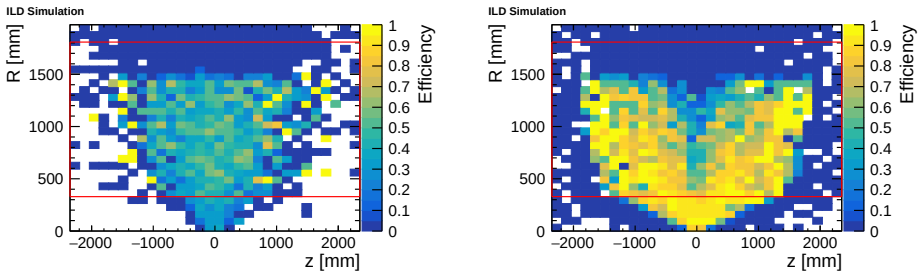

Figure 2: Vertex finding efficiency after the standard selection, but without the cut on the vertex radius, as a function of the true LLP decay vertex position in the detector. The efficiency is shown for the heavy scalar pair-production with $\Delta m_{AH} = 2\,\text{GeV}$ (left) and for the light pseudoscalar production scenario with $m_a = 1\,\text{GeV}$ (right). The TPC volume is shown with the red box.

Table 2: The vertex finding efficiency inside the TPC region obtained in the analysis after different sets of cuts, both for scalars pair-production and light pseudoscalars for all considered scenarios.

Δm_{AH} [GeV]	1	2	3	5
Efficiency (standard) [%]	3	33.2	43.4	51.1
Efficiency (tight) [%]	0.4	28.3	40.7	50.2
m_a [GeV]	0.3	1	3	10
Efficiency (standard) [%]	7.4	48.4	61.7	65.8
Efficiency (tight) [%]	–	47.3	61.7	65.8

"correct" if it was closer than 30 mm from the true vertex. The cut on the vertex radius was removed to indicate differences between reconstruction efficiency in the silicon tracker and inside the TPC. It can be noticed that in case of the soft final state, efficiency within the TPC region tend to be slightly higher, which is thanks to large number of hits produced by the tracks. For the vertices with high-p_T tracks the efficiency is higher for decays in the silicon trackers, because these tracks are highly collimated and the silicon trackers provide better two-track separation.

Total vertex finding efficiencies, for all signal scenarios considered and both standard and tight selections, are summarized in Table 2. In the case of heavy scalars, the efficiency strongly depends on the Z* virtuality which determines the final state boost. The sensitivity to $\Delta m_{AH} = 1\,\text{GeV}$ scenario is suppressed by the $p_T^{vtx} > 1.9\,\text{GeV}$ cut applied to reduce the background from overlay events, while for the rest of scenarios good sensitivity is achieved. For the light LLP, the efficiency decreases with the final state boost, as opposed to the heavy scalar case. In the $m_a = 300\,\text{MeV}$ scenario most of the vertices are poorly reconstructed due to high colinearity and therefore removed by quality cuts. For tight selection, the sensitivity is completely lost because of cuts on the invariant mass smaller than 700 MeV. It is important to note, that for both $\Delta m_{AH} = 1\,\text{GeV}$ and $m_a = 300\,\text{MeV}$ scenarios the reach could be significantly improved by a dedicated approach, with a selection optimized for each type of scenario (i.e. using information about the missing energy or the hard photon).

The vertex finding efficiencies ϵ_{sel} were translated into the expected 95% C.L. limits on the signal production cross section. They were calculated assuming $2\,\text{ab}^{-1}$ of the integrated

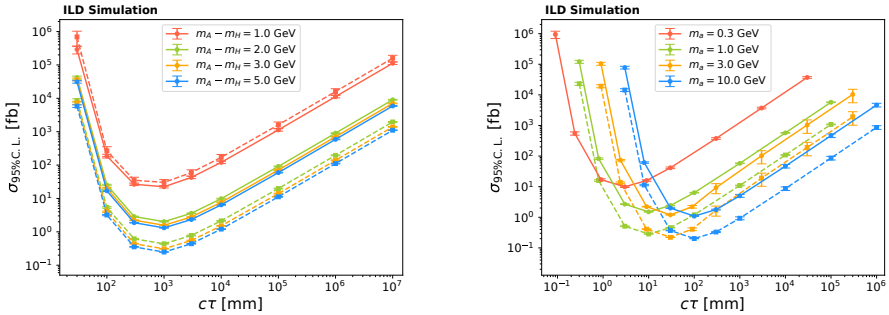

Figure 3: Expected 95% C.L. upper limits on the signal production cross-section for the considered benchmarks and different LLP mean decay lengths, for the scalar pair-production (left) and the light pseudoscalar production (right) at $\sqrt{s} = 250$ GeV. Solid lines corresponds to the standard selection and dashed lines to the tight set of cuts. The uncertainties are statistical.

luminosity, the total estimated number of $1.06 \cdot 10^{12}$ of the overlay events and the background rejection factors from Sec. 3. An event re-weighting using the exponential distribution was also performed to obtain the limits for a range of LLP lifetimes without generating and processing a large number of event samples.

The 95% C.L. limits $\sigma_{95\%\text{C.L.}}$, corresponding to the number $N_{lim} = 1.96\sqrt{N_{bg}}/\epsilon_{sel}$ (assuming $\epsilon_{sel}N_{lim} \ll N_{bg}$), are presented in Fig. 3 as a function of LLP proper decay length $c\tau$. The limits are shown for both sets of cuts and all scenarios considered, for the heavy (left) and light (right) LLP production. In case of the scalar pair-production, limits at the order of femtobarns can be reached in the $c\tau$ range of 0.3-10 m. This can be improved by an order of magnitude with the tight selection for most of scenarios, except for the most challenging $\Delta m_{AH} = 1$ GeV benchmark, for which the limit gets slightly worsened because of the enhanced cuts on a track pair invariant mass. For the light pseudoscalar case, the level of femtobarns is achieved in range of 3-1000 mm of proper decay lengths. That is again improved by an order of magnitude by the tight selection, except for the scenario with the smallest mass, for which the sensitivity is completely lost, as in this case the mass peak is fully below the track pair mass threshold used in the tight selection.

5 Impact of the detector design

Influence of the detector design on the sensitivity to LLP decays to soft final states has also been tested. For that purpose, an alternative ILD design was used, in which the TPC was replaced by an all-silicon outer tracker, taken from the detector model proposed for the Compact Linear Collider (CLICdet) [12]. One barrel layer had to be added and spacing between endcap layers increased in order to fit the ILD geometry. For track reconstruction in the alternative detector model the Conformal Tracking [13] was used, a pattern recognition algorithm designed originally for CLICdet.

Figure 4 presents the track reconstruction efficiency as a function of the true LLP decay vertex distance from the beam axis, for different scenarios with the heavy scalar production. The efficiency is compared for the standard and alternative ILD designs. For decays close to the interaction point, where both detector models are identical, the performance is very similar. However, for higher displacements, the efficiency drops quickly in the case of the

all-silicon tracker (reaching almost zero already at 1 m), while for the baseline ILD design it remains high almost throughout the whole detector volume. The reason is a limited number of layers in the silicon tracker. At least 4 hits are required to reconstruct a track, and the biggest drop in efficiency is visible at the distance of 500 mm, from which only four barrel layers remain. Also, even having 4 hits does not guarantee reconstruction of a high-quality track.

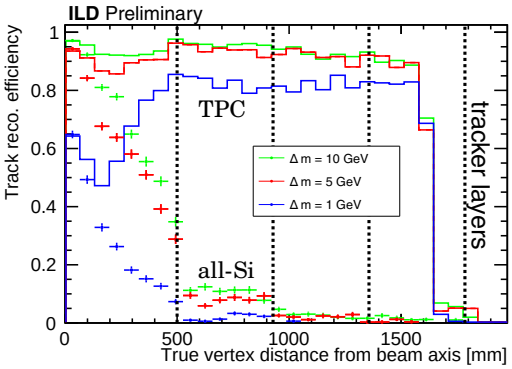

Figure 4: Track reconstruction efficiency as a function of distance from the beam axis for the heavy scalar samples in the all-silicon ILD design (points), compared to efficiency in the baseline TPC-equipped ILD (solid lines). Different colours correspond to particular scalar mass-splitting scenarios in the test samples. Vertical dashed lines show the position of barrel layers of the outer silicon tracker in all-silicon model.

6 Conclusion

We analyze the prospects for detecting neutral LLPs at the ILD experiment with a displaced vertex signature. An experiment-focused approach was used, in which we select benchmarks not fully tested at the LHC, based on their kinematic properties. Two very challenging signatures were studied; the first with a heavy LLP production and a very soft final state, and the opposite one, with high-p_T, almost colinear tracks originating from a displaced vertex. We study background sources both from beam-induced, and hard processes.

Based on expected background levels and the obtained signal selection efficiencies, we find that neutral LLP production could be constrained with the ILD down to the level of 0.1 fb in a wide range of LLP proper decay lengths, 0.003-10 m, depending on the kinematics of the final state. However, it should be noted that the results are based on a very model-independent approach and should be considered conservative; a dedicated approach taking into account particular signal properties would further improve the results.

The impact of the detector design on the sensitivity to LLPs was also tested. The results confirm the expectations that TPC can significantly enhance detector acceptance, and therefore also the reach for LLP decays to soft final states.

Acknowledgements

This study was carried out in the framework of the ILD Concept Group. The work was supported by the National Science Centre (Poland) under OPUS research project

no. 2021/43/B/ST2/01778. We would like to thank the LCC generator working group and the ILD software working group for providing the simulation and reconstruction tools and producing the Monte Carlo samples used in this study. This work has benefited from computing services provided by the ILC Virtual Organization, supported by the national resource providers of the EGI Federation and the Open Science GRID.

References

[1] J. Alimena et al., Searching for long-lived particles beyond the Standard Model at the Large Hadron Collider, J. Phys. G **47**, 090501 (2020), 1903.04497. 10.1088/1361-6471/ab4574

[2] L. Lee et al., Collider Searches for Long-Lived Particles Beyond the Standard Model, Prog. Part. Nucl. Phys. **106**, 210 (2019), [Erratum: Prog.Part.Nucl.Phys. 122, 103912 (2022)]. 10.1016/j.ppnp.2019.02.006

[3] E.S. Group, 2020 Update of the European Strategy for Particle Physics (CERN Council, Geneva, 2020), ISBN 978-92-9083-575-2

[4] P. Bambade et al., The International Linear Collider: A Global Project (2019), 1903.01629.

[5] H. Abramowicz et al. (ILD Concept Group), International Large Detector: Interim Design Report (2020), 2003.01116.

[6] M. Thomson, Particle flow calorimetry and the PandoraPFA algorithm, Nuclear Instruments and Methods in Physics Research Section A: Accelerators, Spectrometers, Detectors and Associated Equipment **611**, 25–40 (2009). 10.1016/j.nima.2009.09.009

[7] J. Klamka, A.F. Zarnecki, Searching for displaced vertices with a gaseous tracker for a future e^+e^- Higgs factory (2024), 2409.13492.

[8] J. Kalinowski et al., Benchmarking the Inert Doublet Model for e^+e^- colliders, JHEP **12**, 081 (2018). 10.1007/JHEP12(2018)081

[9] R. Schäfer et al., Near or far detectors? A case study for long-lived particle searches at electron-positron colliders, Phys. Rev. D **107**, 076022 (2023). 10.1103/PhysRevD.107.076022

[10] S. Agostinelli et al., Geant4 — a simulation toolkit, Nucl. Instrum. Meth. A **506**, 250 (2003). https://doi.org/10.1016/S0168-9002(03)01368-8

[11] ilcsoft – linear collider software, https://github.com/iLCSoft

[12] N. Alipour Tehrani et al., CLICdet: The post-CDR CLIC detector model (2017).

[13] E. Brondolin et al. (CLICdp), Conformal tracking for all-silicon trackers at future electron–positron colliders, Nucl. Instrum. Meth. A **956**, 163304 (2020). 10.1016/j.nima.2019.163304